ISSN 0006-2979, Biochemistry (Moscow), 2024, Vol. 89, No. 8, pp. 1392-1401 © The Author(s) 2024. This article is an open access publication.

Functional Analysis of the Channelrhodopsin Genes from the Green Algae of the White Sea Basin

Olga V. Karpova[1,a]*, Elizaveta N. Vinogradova[1,2], Anastasiya M. Moisenovich[1], Oksana B. Pustovit[1], Alla A. Ramonova[1], Denis V. Abramochkin[1], and Elena S. Lobakova[1]

[1]*Division of Biology, Lomonosov Moscow State University, 119991 Moscow, Russia*
[2]*Genome Center, National Research Center "Kurchatov Institute", 123182 Moscow, Russia*
[a]*e-mail: olgakarpova@ymail.com*

Received March 3, 2024
Revised May 31, 2024
Accepted June 19, 2024

Abstract—Optogenetics, the method of light-controlled regulation of cellular processes is based on the use of the channelrhodopsins that directly generate photoinduced currents. Most of the channelrhodopsin genes have been identified in the green microalgae Chlorophyta, and the demand for increasing the number of functionally characterized channelrhodopsins and the diversity of their photochemical parameters keeps growing. We performed the expression analysis of cation channelrhodopsin (CCR) genes in natural isolates of microalgae of the genera *Haematococcus* and *Bracteacoccus* from the unique Arctic Circle region. The identified full-length CCR transcript of *H. lacustris* is the product of alternative splicing and encodes the Hl98CCR2 protein with no photochemical activity. The 5′-partial fragment of the *B. aggregatus* CCR transcript encodes the Ba34CCR protein containing a conserved TM1-TM7 membrane domain and a short cytosolic fragment. Upon heterologous expression of the TM1-TM7 fragment in CHO-K1 cell culture, light-dependent current generation was observed with the parameters corresponding to those of the CCR. The first discovered functional channelrhodopsin of *Bracteacoccus* has no close CCR homologues and may be of interest as a candidate for optogenetics.

DOI: 10.1134/S0006297924080030

Keywords: channelrhodopsins, green algae, photo-induced current, optogenetics

INTRODUCTION

Channelrhodopsins are a special group of integral membrane retinal-binding proteins, which carry out direct passive ion transport in response to photoactivation, unlike other rhodopsins (in particular, visual ones) that regulate ion channels indirectly through activation of enzymatic cascades [1]. In nature, channelrhodopsins are mainly found in motile phototrophic organisms, the microalgae Chlorophyta and Cryptophyta, where they act as the phototaxis photoreceptors. For the first time, photoelectric response in phototaxis was shown *in vivo* in the cells of green alga *Haematococcus pluvialis* [2] and subsequently studied in detail in the green alga *Chlamydomonas reinhardtii* [3]. The identified photoreceptors CrChR1 and CrChR2 of *C. reinhardtii* are cation channelrhodopsins (CCRs), which differ both in the photoinduction parameters and in the kinetics of photoelectric response [3, 4]. It is assumed that the main role in phototaxis is played by CrChR2, while CrChR1 is involved in protection from high-intensity light.

Due to unique features, channelrhodopsins are widely used in optogenetics, a method of light-controlled regulation of processes within cells. In the optogenetic experiment, with heterologous expression in the target cells, the genes of channelrhodopsins and ion pumps with specificity for cations and anions provide depolarization and hyperpolarization of the cell membrane and thus allow to regulate neuronal activity [5]. Despite the vast progress in the search for new

Abbreviations: RACE, rapid amplification of cDNA ends.

* To whom correspondence should be addressed.

channelrhodopsin genes by genomic analysis methods, the number of genes encoding proteins with experimentally confirmed functional activity is still very limited [6]. As a result, the cation channelrhodopsin CrChR2 of green alga *C. reinhardtii* remains so far the most studied and employed in various modifications for optogenetic research.

Our work is aimed at finding new genes of channelrhodopsins in the unicellular algae Chlorophyta and Cryptophyta of the White Sea basin and is based on the collection of the microalga natural isolates NAMSU (https://depo.msu.ru/open/public/en/search?collection=algabiotech), created at the Bioengineering Department, Division of Biology, Lomonosov Moscow State University. The presented data expand the results of our previous study focused on finding novel CCRs in the green algae *Haematococcus* and *Bracteacoccus*. Earlier, using the PCR-test developed in our laboratory, presence of the CCR gene (*34CCR*) in the microalgae of the *Bracteacoccus* genus was first shown; the CCR genes (*37CCR* and non-homologous *98CCR1*, *98CCR1-1* genes) corresponding to the already identified *Haematococcus lacustris* CCR genes were also detected in two *H. lacustris* isolates [7]. Thus, this PCR test was effective not only for analysis of a taxonomic group for the presence of CCR genes, but also for analysis of the multigene CCR families.

To study expression of the detected CCR genes of *Haematococcus* and *Bracteacoccus*, their transcripts were obtained, structural analysis of their protein products (Hl98CCR2 and Ba34CCR) was carried out, and functional activity of Hl98CCR2 and Ba34CCR was determined during heterologous expression in the culture of Chinese hamster cells CHO-K1. We have shown that Hl98CCR2 and Ba34CCR proteins contain 7 conserved membrane regions (TM1-TM7) with transmembrane localization and are capable of forming homodimers, which is typical for the spatial structure of channelrhodopsins. In electrophysiological experiments with transfected CHO-K1 cells using the patch-clamp method, it was shown that the expressed Ba34CCR protein is capable of light-dependent current generation and is comparable to the cation channelrhodopsin CrChR2 of *C. reinhardtii* in its parameters. Thus, we have discovered and characterized for the first time a functional cation channelrhodopsin from the green microalga *Bracteacoccus*.

MATERIALS AND METHODS

Origin of green algae strains (Chlorophyta) and cultivation conditions were as previously detailed [7]. To isolate total RNA, actively growing cultures of *H. lacustris* NAMSU-BM-7/15 and *B. aggregatus* NAMSU-BM-5/15 were cultivated in a BG-11 medium with incubation for 1-2 weeks at 25°C and illumination with white light at the intensity of 40 μmol PAR quanta $m^{-2} \cdot s^{-1}$.

RNA isolation and production of CCR-specific transcripts. Total RNA was isolated from 5-10 ml of cultures using a RNeasy plus kit (Qiagen, USA). For RNA extraction, samples (~100 mg of wet weight) were lysed by mechanical destruction in a FastPrep-24™ 5G disintegrator (MP Biomedicals, USA) in the presence of Lysing Matrix type A microbeads. 250 ng of RNA were taken to prepare cDNA; full-length transcripts were prepared by rapid amplification of cDNA ends (RACE) using a Mint-RACE kit (Evrogen, Russia). The obtained PCR products were analyzed by electrophoresis in a 1% agarose gel and eluted from the gel with a Cleanup Mini kit (Evrogen). Further, PCR products were sequenced using Sanger method (Center of the collective use "Genome" at EIMB RAS, Russia), the sequences were aligned and matched by homology sites (BLASTn, NCBI).

Structural and functional characteristics of translated CCR-specific transcript products and 3D modeling. To analyze the translated amino acid sequences of the obtained CCR transcripts and to determine the homology with the previously identified Chlorophyta CCR proteins, we applied the CLUSTAL Omega multiple alignment method (https://www.ebi.ac.uk/Tools/msa/clustalo/). 3D modeling was performed using the SWISS-MODEL program (https://swissmodel.expasy.org/) with the crystal structure of CrChR2 *C. reinhardtii* as a template.

Heterologous expression of rhodopsins in CHO-K1 cell culture. *Construction of expression plasmids.* For expression in mammalian cells, nucleotide sequences of Hl98CCR2 (full reading frame, 350 a.a.) and Ba34CCR (1-295 a.a.) transcripts were codon-optimized (GeneArt; Thermo Fisher Scientific, USA); chemical synthesis of both genes was performed (Evrogen) and they were subcloned into a pcDNA3.1 eYFP expression vector [8] at BamHI and NotI restriction sites.

Transfection of expression plasmids into CHO-K1 cell culture. An immortalized ovary epithelial cell line of Chinese hamster *Cricetulus griseus* (Chinese hamster ovary cells) was used for heterologous expression of Ba34CCR and Hl98CCR2 proteins. Transfection of cells with pcDNA3.1 eYFP. Ba34CCR and pcDNA3.1 eYFP. Hl98CCR2 expression vectors was performed using a Lipofectamine® LTX with Plus™ Reagent (Thermo Fisher Scientific). Marker of successful transfection was cell fluorescence excited with 490-nm light. Transfected cells were maintained under standard culture conditions in a DMEM/F12 culture medium (Gibco, Thermo Fisher Scientific) supplemented with 10% fetal bovine serum (FBS; HyClone, USA), 2 mM glutamine (Sigma-Aldrich, USA), and 100 μg/ml penicillin-streptomycin (Gibco, Thermo Fisher Scientific) at 37°C under

21% O_2 and 5% CO_2. Twenty-four hours after transfection, 1 μM R2500 trans-retinal (Sigma-Aldrich) was added to the culture medium.

Fluorescence microscopy of expressed rhodopsins. To determine localization of the expressed proteins Ba34CCR and Hl98CCR2, transfected CHO-K1 cells were treated with fluorescent dyes specific for cytoplasmic membranes (CellBrite Red; Biotium, UK) and nuclei (Hoechst 33342, Thermo Fisher Scientific). For that, cells were incubated with 10 μM CellBrite Red in normal medium containing 1% DMSO and 5 μg/ml Hoechst 33342 for 15 min, washed twice with PBS and once with DMEM. Intravital images were obtained using an Eclipse Ti-E microscope life support system with a confocal A1 module (Nikon Corporation, Japan) and Apo TIRF 63×/1.49 lens. All images were captured using the same dynamic range settings.

Photoelectric activity determination for Ba34CCR and Hl98CCR2 rhodopsins. Electrophysiological experiments were performed 48 h after transfection. Photo-induced current of Hl98CCR2 (I_{98}) or Ba34CCR (I_{34}) was recorded in the transfected CHO-K1 cells using whole-cell patch-clamp technique. An Axopatch 200A amplifier (Molecular Devices, USA) was used.

A coverslip with CHO-K1 culture was placed in an experimental chamber and perfused at room temperature (23 ± 0.5°C) with a solution of the following composition: 150 mM NaCl; 5.4 mM KCl; 1.8 mM $CaCl_2$; 1.2 mM $MgCl_2$; 10 mM glucose; 10 mM HEPES (pH 7.6). Only cells emitting green fluorescence upon exposure to 490-nm excitation light were selected for examination. 2-2.5 MOhm patch pipettes were made of borosilicate glass (Sutter, USA) and filled with a solution of the following composition: 140 mM KCl; 1 mM $MgCl_2$; 5 mM EGTA; 4 mM MgATP; 10 mM HEPES; 0.03 mM Na_2GTP (pH 7.2). Before the start of current recording, the pipette capacity, test cell capacity, and access resistance were compensated. Both transmitted light and 490-nm light were also turned off. In data processing, current amplitudes were normalized to cell capacity and expressed in pA/pF.

To record I_{98} and I_{34}, two different protocols were used to study dependence of the current density on intensity of the excitation light and current-voltage dependence, respectively. Both protocols used a holding potential of –60 mV. In the first protocol, the potential value was 0 mV, and then 490-nm light was turned on for 1 s; the resulting outward current was photo-induced, since there is no leakage current at a potential of 0 mV. Light intensity of 1, 2, 3, 5, 10, 20, 50, and 100% of the maximum possible for a CoolLED pE-100 light source (CoolLED, UK) was sequentially applied. Absolute values of light intensity were determined using a PM160T sensor (Thorlabs, USA). In the second protocol, the potential was changed stepwise from the holding potential to values from –100 to 60 mV with a step of 20 mV for 2 s, while during each of the steps 490-nm light was turned on with intensity of 50% of the maximum for 1 s. The photo-induced current in this case was calculated as the difference between the current in the presence and absence of excitation light at each of the membrane potential values. In both cases, the maximum (peak) value of the light-induced current, as well as the current plateau level (average current value in the range of 500-1000 ms of light supply) were measured. Statistical processing of the results and plotting were performed using GraphPad Prism 7. The data are presented as a mean ± standard error of the mean.

RESULTS

Obtaining CCR transcripts from green microalgae *Haematococcus* and *Bracteacoccus*. Total RNA of *Haematococcus* and *Bracteacoccus* was isolated according to the method described in Materials and Methods section, after which the CCR-specific transcripts were prepared by rapid amplification of cDNA ends (RACE). The RACE procedure was performed sequentially over 3 rounds of PCR using primers presented in Table 1.

As a result, a full-length transcript of the CCR gene of *H. lacustris* NAMSU-BM-7/15 and a 5′-partial fragment of the CCR transcript of *B. aggregatus* NAMSU-BM-5/15 gene were obtained.

The CCR transcript of *Haematococcus* was not the product of any of the genes we have identified previously [*98CCR1* (GenBank: ON643073.1) and *98CCR1-1* (GenBank: ON643074.1)], as it was expected initially, but subsequently we identified it as the *98CCR2* gene (data not shown). Homology between the obtained Hl98CCR2 transcript (GenBank: PP103616) and the *98CCR1* gene is 81.9%.

We were unable to obtain a full-length transcript of the *Bracteacoccus* NAMSU-BM-5/15 CCR gene, but the 5′-partial fragment of the Ba34CCR transcript (GenBank: PP103617) was determined to be a product of the previously identified *34CCR* gene (GenBank: ON643076.1). As of now, the Ba34CCR transcript has been entirely mapped to the genomic sequence; it was found that the corresponding gene region contains 4 introns.

Structural and functional characteristics of Hl98CCR2 and Ba34CCR protein products and 3D modeling. To determine structural and functional characteristics, homology modeling was used by aligning the translated amino acid sequences of native CCR transcripts obtained by homologous cloning [9] or identified by the transcriptome analysis [3, 10, 11].

Figure 1 shows alignment of the translated amino acid sequences of the *Haematococcus* CCR gene products and their native transcripts. As shown in Fig. 1,

Table 1. PCR primers for amplification of *Haematococcus* and *Bracteacoccus* CCR cDNA

RACE, rounds		Gene-specific primers	
		Haematococcus	*Bracteacoccus*
RACE 5′	round 1	CCR_rev: CCCTTGGGMACDGTRTGGTA	34CCR-ORF_rev: ACCACAGTGTGCGCGACGA
	round 2	Hae-687_rev: GTTGGGTGGACTCATAGCCGCAG	34CCR1_rev: CCGTAGCACAAACCAATGCAGA
	round 3	98CCR1_rev: GGTGCGTTTGGAGTAGTCATCC	34CCR2_rev: CAAACCCGTCAGGTTGGACAAG
RACE 3′	round 1	CCR_fwd: YGGHTGGGARGAGRTBTACGT	34CCR1_fwd: CTTGTCCAACCTGACGGGTTTG
	round 2	Hae-536_fwd: GGAGTGGTTACTGTCATGCCCAGT	34CCR2_fwd: TCTGCATTGGTTTGTGCTACGG
	round 3	98CCR1_ fwd: GGATGACTACTCCAAACGCACC	34CCR3_fwd: TCGTCGCGCACACTGTGGT

Hl37CCR, Hl98CCR1, Hl98CCR2, and Hl98CCR1-1 products contain 7 membrane spirals and conserved amino acid residues typical of channelrhodopsins. There is a retinal binding site, Lys257, Glu (82, 83, 101, and 123), as well as Glu90 that determines specificity of the rhodopsins cation transfer [1, 6]. Glu235 and Ser245, involved in determining the pH dependence of the spectral characteristics of CCR proteins, are also conserved. Hou et al. [9] showed for the *Mesostigma viride* CCR that replacing Ser at 245 position with Glu resulted in the complete loss of channel activity. Ser321 is the only CrChR2 protein phosphorylation site that is located in the conserved region of the cytosolic loop adjacent to the TM7 transmembrane domain (helix 7). We were unable to determine presence of a phosphorylation site in Hl98CCR2 because the 3′-end of the transcript exhibited low homology.

The closest homologue of the Ba34CCR partial transcript product of *B. aggregatus* NAMSU-BM-5/15 is CrChR2 *C. reinhardtii* (59.2% identity at 73% sequence coverage). Figure 2 shows alignment of the translated amino acid sequences of Ba34CCR and native CCR transcripts from different *Chlamydomonas* species. The Ba34CCR transcript encodes the entire TM1-TM7 membrane fragment with all conserved amino acid residues and a unique Lys-enriched fragment lacking homology.

Thus, based on the primary structure analysis of the Hl98CCR2 and Ba34CCR native transcript products, we conclude that the encoded proteins contain 7 conserved membrane regions (TM1-TM7), along with the functionally significant amino acid residues characteristic of the channelrhodopsins. 3D models of Hl98CCR2 and Ba34CCR proteins also demonstrated a spatial structure typical of channelrhodopsins: transmembrane localization of the TM1-TM7 fragment and formation of homodimers (Fig. 3). These results allow identification of Hl98CCR2 and Ba34CCR proteins as channelrhodopsins and indicate their possible functional activity.

Determination of functional activity of Ba34CCR and Hl98CCR2 channelrhodopsins. This task was performed using an approach first proposed by Nagel et al. [12, 13]. When expressed in *Xenopus laevis* oocytes or in animal cells (HEK293, BHK), channelrhodopsins *C. reinhardtii* were shown to function as light-dependent cation channels. Moreover, not only full-length proteins, but also their TM1-TM7 fragments were shown to be capable of photoinducing ion currents, which could be detected by patch-clamp method. Thus, the experimental task of this step was to determine photoelectric activity of Ba34CCR and Hl98CCR rhodopsins during heterologous expression in mammalian cells.

Heterologous expression of Ba34CCR and Hl98CCR2 in the culture of CHO-K1 cells. For expression in mammalian cells, Hl98CCR2 and Ba34CCR codon-optimized cDNA nucleotide sequences were subcloned into the pcDNA3.1 eYFP expression vector as described in Materials and Methods section, where the analyzed genes were transcribed from the highly efficient P_CMV promoter of cytomegalovirus and translated in the same frame with YFP (a fluorescence marker). The obtained pcDNA3.1 eYFP. Ba34CCR and pcDNA3.1 eYFP. Hl98CCR2 expression plasmids were used to transfect an immortalized Chinese hamster ovary epithelial cell line CHO-K1. The level of expression and intracellular localization of Ba34CCR-YFP and Hl98CCR2-YFP protein conjugates in the transfected cells were determined by intravital fluorescence microscopy after treatment of the cells with specific dyes.

The results of a typical experiment are shown in Fig. 4. Comparison of the intrinsic fluorescence of the Ba34CCR and Hl98CCR2 YFP conjugates with the cell staining with CellBrite Red determines clearly localization of the expressed proteins in the cytoplasmic membrane. Expression level of the full-length Hl98CCR2 protein was reproducibly observed to be below the expression level of the Ba34CCR protein TM1-TM7 membrane fragment.

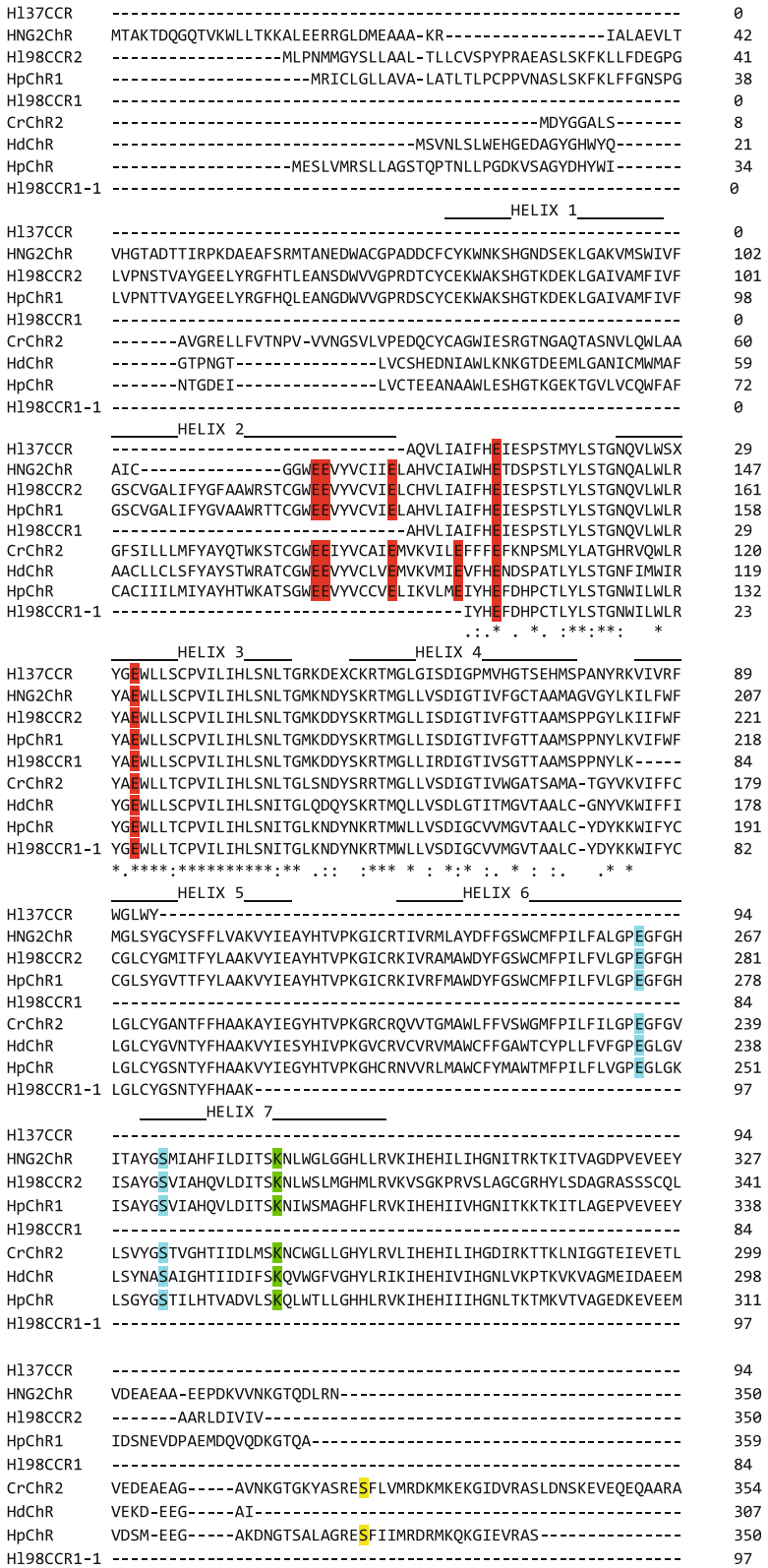

Fig. 1. Alignment of translated amino acid sequences (CLUSTAL Omega) of the *Haematococcus* CCR gene products and their native transcripts. Hl37CCR, 94 a.a.; Hl98CCR1, 84 a.a.; Hl98CCR1-1, 97 a.a., fragments of *H. lacustris* CCR genes [7]; Hl98CCR2, 350 a.a., native transcript of the gene *98CCR2*; native transcripts: HpChR1 *H. pluvialis (lacustris)*, 677 a.a. (GenBank: JN596950 [9]); HpChR *H. pluvialis (lacustris)*, 449 a.a [11]; HNG2ChR *Haematococcus* sp. NG2 , 350 a.a [11]; HdChR *H. droebakensis*, 307 a.a. (GenBank: KF992059 [10]); CrChR2 *C. reinhardtii*, 737 a.a. (GenBank: AF508966 [3]). Functionally significant amino acid residues (numbering corresponds to CrChR2) are highlighted by the following colors: Glu (82, 83, 90, 97, 101, and 123) – red; Glu235 and Ser245 – light blue; Lys257 – green; Ser321 – yellow.

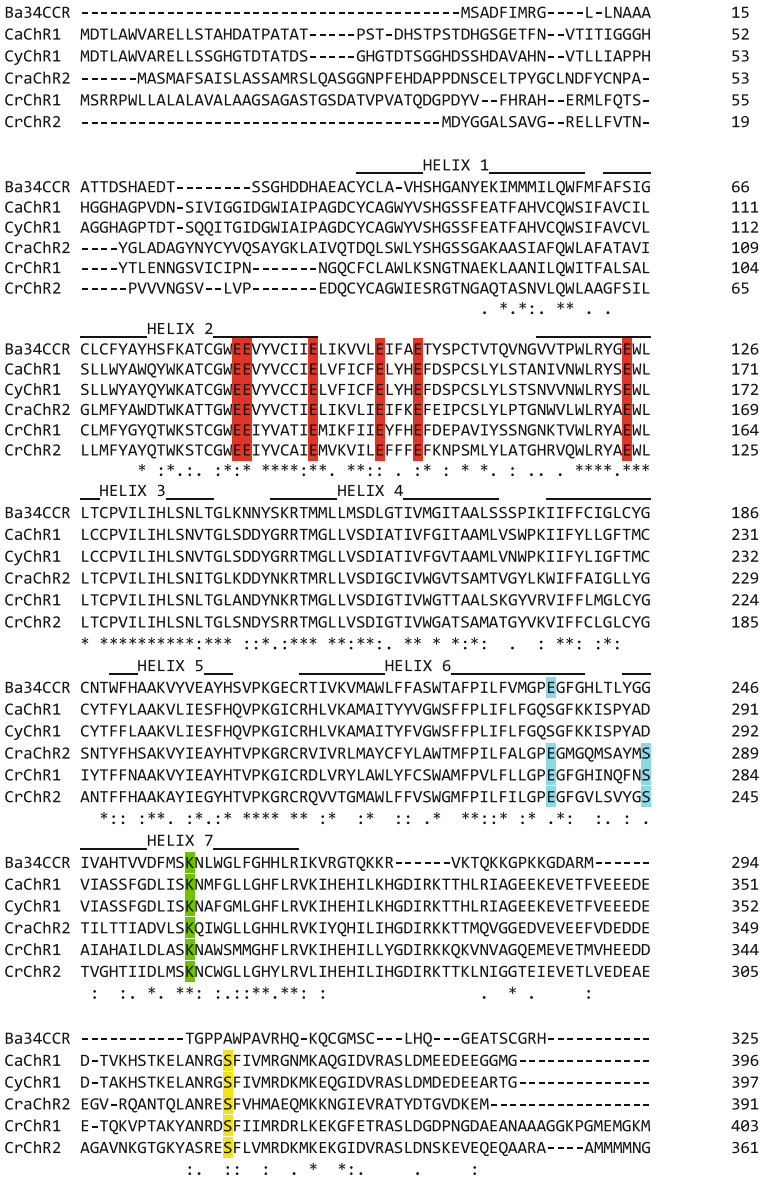

Fig. 2. Alignment of translated amino acid sequences (CLUSTAL Omega) of native CCR transcript products from *Bracteacoccus* and *Chlamydomonas*. Ba34CCR: partial transcript of the *34CCR* gene *B. aggregatus* NAMSU-BM-5/15, 325 a.a.; native transcripts: CrChR2 *C. reinhardtii*, 737 a.a. (GenBank: AF508966 [3]); CaChR1 *C. augustae*, 715 a.a. (GenBank: JN596951 [9]); CraChR2 *C. raudensis*, 635 a.a. (GenBank: JN596949 [9]); CyChR1 *C. yellowstonensis*, 717 a.a. (GenBank: JN596948 [9]). Functionally significant amino acid residues (numbering corresponds to CrChR2) are highlighted by the following colors: Glu (82, 83, 90, 97, 101, and 123) – red; Glu235 and Ser245 – light blue; Lys257 – green; Ser321 – yellow.

Determination of photoelectric activity of the expressed Ba34CCR and Hl98CCR2 rhodopsins. Figure 5 shows the results of experiments with CHO-K1 cells transfected with plasmids pcDNA3.1 eYFP. Ba34CCR and pcDNA3.1 eYFP. Hl98CCR2.

In the cells expressing Hl98CCR2, the 490-nm light in the absence of transmitted light at a membrane potential of –20 mV did not contribute to generation of the pronounced I_{98} inward or outward current (Fig. 5a), or this current was at the noise level. Therefore, dependence of the current on intensity and membrane potential could not be analyzed.

In the cells expressing Ba34CCR, the 490-nm light in the absence of transmitted light at a membrane potential of –20 mV contributed to the I_{34} incoming current generation (Fig. 5b), which at the light intensity values from 0.67 mW/mm^2 and higher had a pronounced peak component that decayed within 20-65 ms, as well as a stationary component (plateau). The mean value of time constant for the peak I_{34} decay at –60 mV was 11.3 ± 0.78 ms (n = 14). Mean value of the I_{34} plateau current deactivation with the light turned off was 25.5 ± 2.5 ms (n = 14). The observed dependence could be explained by

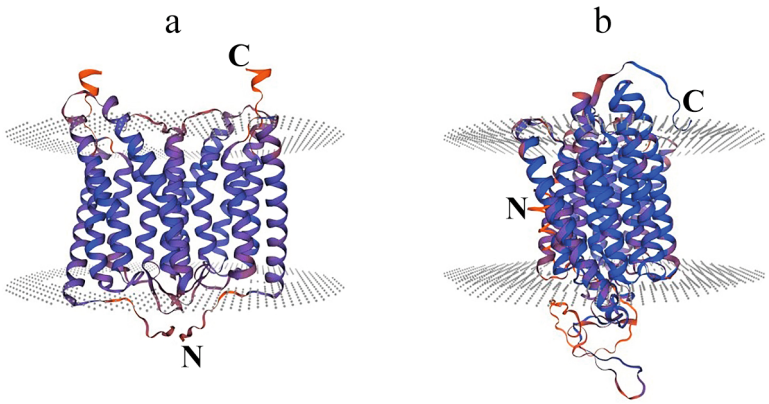

Fig. 3. 3D models of identified Ba34CCR (a) and Hl98CCR2 (b) channelrhodopsins (SWISSMODEL). The crystal structure of CrChR2 *C. reinhardtii*, 6eid.1.A, is used as a template. N and C indicate localization of polypeptide chain ends. Color code (red to blue) shows the level of homology with the template.

desensitization of the channels formed by the Ba34CCR protein.

I_{34} peak and plateau current amplitudes demonstrated positive dependence on the 490-nm light intensity up to 2.8 mW/mm^2. Further increase in the light intensity resulted in the decrease in the amplitude of the peak current (Fig. 5, b and c). At the negative membrane potential values, both peak current and plateau current have an inward direction. When crossing the 0-mV level and when the membrane potential is positive, the current direction changes to the outward one (Fig. 5d). Thus, 0 mV is the reversible potential for I_{34} current under the experimental conditions indicated in the Materials and Methods section.

DISCUSSION

With the development of optogenetic studies, the demand for a wider variety of channelrhodopsins' functional characteristics to solve various experimental problems is growing significantly. As a result, researchers are still turning to the analysis of microalgae Chlorophyta, a huge group of phototrophic organisms with a variety of forms and habitats, in search of new candidate genes for optogenetics. According to the data available in 2021 [6], testing of 56 CCR genes in Chlorophyta (out of 164 identified ones) revealed functional activity of 40 genes; there are also data on first identification and functional activity of the anion channelrhodopsin (ACR) genes in green algae [11]. We considered it relevant to analyze the genes of channelrhodopsins of the natural microalgae isolates of the genera *Haematococcus* and *Bracteacoccus* from the White Sea basin and determine functional activity of their protein products.

Previously, we identified 2 non-homologous CCR genes in the microalga *H. lacustris* NAMSU-BM-7/15 (*98CCR1* and *98CCR1-1*), however, a full-length Hl98CCR2 transcript obtained and characterized in the expression analysis was not the product of any of the abovementioned genes. Thus, by rapid amplification of cDNA ends (RACE) using degenerate primers, we were able to detect the third CCR gene of *H. lacustris* NAMSU-BM-7/15.

Since 7 predicted *H. lacustris* CCR genes have already been deposited in the GenBank database, it seemed relevant to determine homologues of the *98CCR1-1*, *98CCR1*, and *98CCR2* genes identified in the *H. lacustris* NAMSU-BM-7/15 strain. According to our data, the *98CCR1-1* gene is mapped in a single region of the genome containing (presumably) the channelrhodopsin gene (GenBank: GFH21497). The *98CCR1* gene exhibits the same homology (85% identity at 95% sequence coverage) with two regions containing channelopsin 1 genes (GenBank: GFH25618 and GFH12230). The *98CCR2* gene and the Hl98CCR2 transcript, respectively, are mapped in the vast 8-kbp region of the BLLF01000737 contig, encoding the channelopsin 1 gene (GenBank: GFH14526). However, it is noteworthy that the open reading frame of the Hl98CCR2 does not correspond to the model assembly of the GFH14526 protein. Based on these results, we conclude that the native Hl98CCR2 transcript is one of the alternative splicing variants.

In this regard, we used the native CCR transcripts *Haematococcus* identified in the transcriptomes or obtained by homologous cloning for comparative analysis of the Hl98CCR2 transcript protein product (Fig. 1). It is noteworthy that the full-length Hl98CCR2 transcript encodes a conserved TM1-TM7 membrane fragment with a short Ser-enriched hydrophilic region with a total size of 350 a.a. In contrast, all native CCR transcripts, as well as 5 of the 6 predicted full-length *H. lacustris* CCR genes, encode giant proteins of ~700 a.a. including cytosolic sequences. Notably, the identified Hl98CCR2 is the product of a single "short" predicted gene (GenBank: GFH14526). It remains

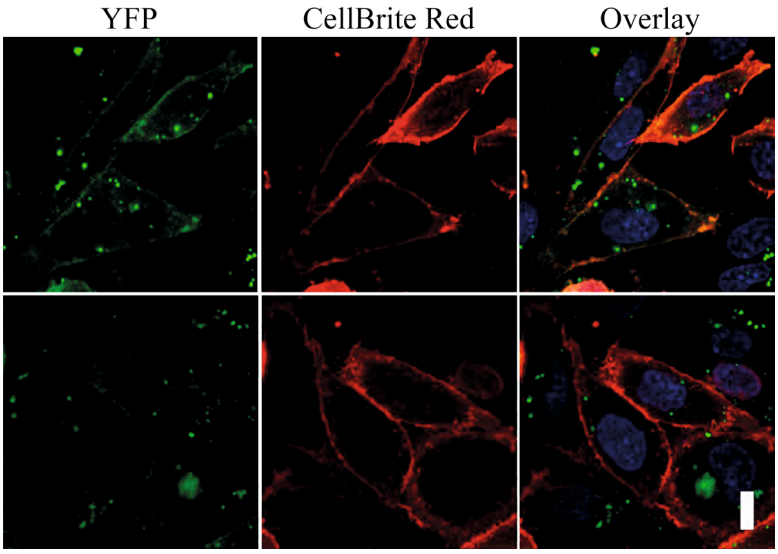

Fig. 4. Examination of localization of the expressed Ba34CCR and Hl98CCR2 rhodopsins in CHO-K1 cells by intravital confocal microscopy: Ba34CCR-YFP (upper row) and Hl98CCR2-YFP (lower row). Cell membranes are stained with CellBrite Red; nuclei are stained with Hoechst 33342. Scale bar: 10 μm.

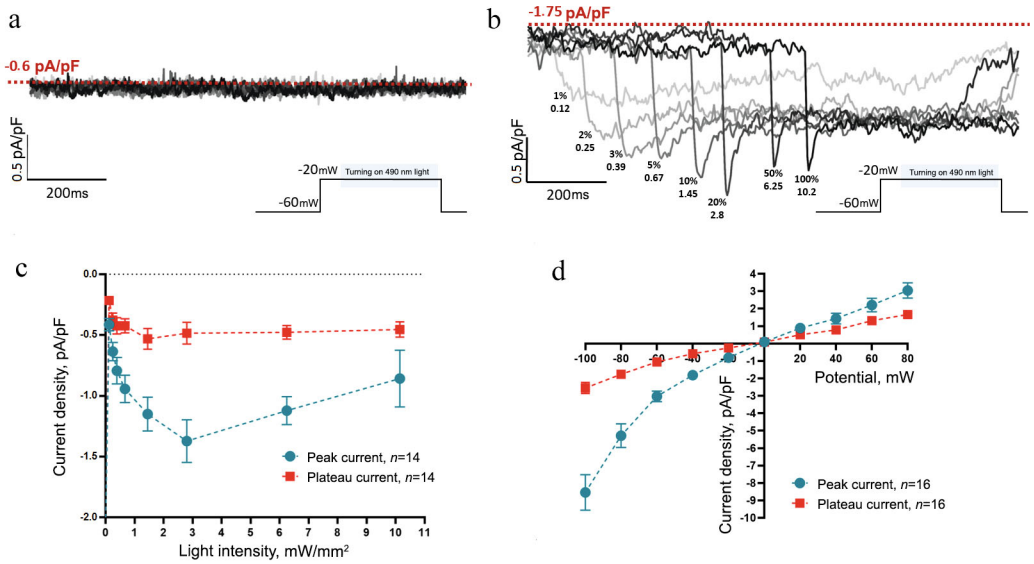

Fig. 5. Characterization of currents generated by Ba34CCR and Hl98CCR2 proteins during the expression in CHO-K1 cells. a) Representative example of original Hl98CCR2 current records (I_{98}) induced by 490-nm light at –20 mV. b) Representative example of original Ba34CCR current records (I_{34}) of different intensities induced by the 490-nm light (intensity is indicated at the peak of each of the curves as a percentage of the maximum, in absolute values of mW/mm^2), at a potential level of –20 mV. c) Dependence of I_{34} peak current and I_{34} plateau current on the 490-nm light intensity. d) Voltage-current curves of I_{34} peak current and stationary current (plateau) of the 490-nm light-induced at 50% of maximum intensity (6.25 mW/mm^2).

unclear why the dominant CCR protein of *H. lacustris* NAMSU-BM-7/15 contains only the TM1-TM7 membrane fragment, and what conditions required for expression of the full-length CCR proteins with regulatory cytosolic regions [14]. The Hl98CCR2 membrane integral protein contains all functionally significant amino acid residues, characteristic of CCR proteins, and forms dimers, but does not show photoelectric activity during heterologous expression in animal cells under standard conditions (Fig. 5a). So far, we do not exclude that, possibly, the Hl98CCR2 protein requires other conditions for generation of photocurrents (absorption spectrum, pH), however, it is worth to mention that its closest homologue and the only tested CCR protein of *H. lacustris*, HpChR1 (85% identity) also does not demonstrate photoelectric activity [9]. Moreover, among the CCR transcripts of *Haematococcus*, only the transcript from *Haematococcus droebakensis* was confirmed to have a functional protein product, HdChR [10].

The product of the *34CCR* gene, Ba34CCR, is of great interest, since it is the first identified channelrhodopsin in the microalga of the *Bracteacoccus* genus. We were able to obtain the 5′-partial transcript fragment of the CCR gene *B. aggregatus* NAMSU-BM-5/15, which encodes a TM1-TM7 membrane fragment and a short Lys-enriched region that does not have any homology. The Ba34CCR protein shows a low level of homology with the channelrhodopsins of Chlorophyta: the closest homologue is CrChR2 *C. reinhardtii* (59% identity). According to the results of 3D modeling, the Ba34CCR protein has transmembrane localization and forms homodimers, which is characteristic of channelrhodopsins (Fig. 3). All known CCR transcripts of *Chlamydomonas* encode proteins of 650-750 a.a. containing a cytosolic fragment along with the membrane fragment TM1-TM7 [9]. It is likely that the full-length Ba34CCR product also belongs to this class of proteins.

During the heterologous expression of the TM1-TM7 fragment of the Ba34CCR protein (1-295 a.a.) in CHO-K1 cell culture, its effective accumulation in the cytoplasmic membrane has been observed (Fig. 4). We also performed electrophysiological experiments using the patch-clamp technique and showed that current generation (I_{34}) occurs in the cells expressing Ba34CCR in response to illumination with the 490-nm light (Fig. 5, b-d).

Since the action spectrum of Ba34CCR rhodopsin has not been studied at this stage, we consider the results obtained as preliminary, and their comparison with the available detailed electrophysiological characteristics of channelrhodopsins CrChR1 and CrChR2 is only partially possible. Nevertheless, it is obvious that the I_{34} photo-induced current is significantly closer in its properties to the current generated by the CrChR2 compared to the CrChR1 rhodopsin current. Like the CrChR2 current [13], I_{34} is subjected to desensitization (inactivation): under the constant supply of excitation light, it weakens spontaneously, plateauing for several tens of milliseconds. On the contrary, for the current generated by the CrChR1, desensitization is uncharacteristic [12].

The data published in a recent work by Hososhima et al. [15] allow comparing amplitude and kinetic characteristics of the current generated by the CrChR2 with I_{34}, considering that CrChR2 data were obtained using heterologous expression in another cell line (ND7/23). The cells expressing CrChR2, when irradiated with the light at intensity of 2.7 mW/mm^2, generated a current at holding potential of –60 mV with peak density of 32 ± 3.2 pA/pF, decreasing to the plateau level of 12 ± 1.1 pA/pF [15]. In our experiments, light of almost the same intensity (2.8 mW/mm^2) was provided at holding potential of –20 mV, however, considering the known voltage-current dependence of the I_{34} (Fig. 5d), it is possible to estimate approximately the I_{34} peak value at –60 mV as 3.7 pA/pF, and the plateau current value as 1.06 pA/pF. Thus, the CrChR2 is able to generate approximately 10 times more current than Ba34CCR, when irradiated with the light of same intensity at 470 nm and 490-nm, respectively. On the other hand, the plateau current value is approximately 37.5% of the peak current value for CrChR2 [15] and 35% for I_{34}. Hence, the CrChR2 and Ba34CCR currents hardly differ in this parameter.

Kinetic characteristics of the I_{34} are comparable with those of the CrChR2 current. The plateau current deactivation time constant occurring after turning off the 490-nm light was 25.5 ± 2.5 ms (n = 14) for I_{34}, while the CrChR2 current, according to Hososhima et al. [15], deactivates 2 times faster (τ_{off} = 12.2 ± 0.69 ms). Inactivation of the I_{34} peak component, to the contrary, occurs several times faster (τ = 11.3 ± 0.78 ms; n = 14) than the estimated inactivation time for the CrChR2 current (~63 ms).

The current generated by the CrChR2 has a reversion potential of ~0 mV with an ion composition of the external environment close to that used in our study [13]. Moreover, if at potentials close to 0 mV (from –40 to 40 mV), the voltage-current dependence of this current is close to linear, then with stronger hyperpolarization, dependence of the inward current on the potential becomes close to exponential. Exactly the same type of voltage-current dependence is characteristic of I_{34}. Unlike the CrChR1 current with exclusively proton nature, the CrChR2 current is the mixed cation current. That is due to indiscriminate permeability of the CrChR2 for various cations, including bivalent ones [13]. This is the reason for the zero-reversion potential of this current under standard physiological conditions. Further experiments with variations in the ion composition of the external and intracellular solution will reveal whether the I_{34} current is also a non-selective cation current.

Acknowledgments. The authors express gratitude to T. A. Fedorenko (Lomonosov Moscow State University) for providing cultures and cultivation recommendations, to the MIPT Aging Center (Dolgoprudny) for the provided expression vector pcDNA3.1 eYFP, as well as to E. G. Maksimov (Lomonosov Moscow State University) for the provided radiation intensity meter. For this study we used equipment purchased within the task of the “Moscow University’s Development Program until 2020” and the equipment of M. V. Lomonosov Moscow State University Center of the collective use.

Contributions. E.S.L., O.V.K., and D.V.A. supervised the study and came up with the concept; E.N.V., O.V.K., A.M.M., O.B.P., and A.A.R. conducted experiments; E.S.L., O.V.K., and D.V.A. discussed the study results; O.V.K. and D.V.A. prepared the manuscript; E.S.L. and D.V.A. edited the manuscript.

Funding. This work was financially supported by the Ministry of Science and Higher Education of the Russian Federation under the agreement no. 075-15-2021-1396 of 26.10.2021. DNA sequencing was carried out as part of the State Budget project of the Kurchatov Institute Research Center.

Ethics declaration. This work does not describe any studies involving humans or animals as objects performed by any of the authors. The authors of this work declare that they have no conflicts of interest.

Open access. This article is licensed under a Creative Commons Attribution 4.0 International License, which permits use, sharing, adaptation, distribution, and reproduction in any medium or format, as long as you give appropriate credit to the original author(s) and the source, provide a link to the Creative Commons license, and indicate if changes were made. The images or other third-party material in this article are included in the article's Creative Commons license, unless indicated otherwise in a credit line to the material. If material is not included in the article's Creative Commons license and your intended use is not permitted by statutory regulation or exceeds the permitted use, you will need to obtain permission directly from the copyright holder. To view a copy of this license, visit http://creativecommons.org/licenses/by/4.0/.

REFERENCES

1. Govorunova, E. G., Sineshchekov, O. A., and Spudich, J. L. (2022) Emerging diversity of channelrhodopsins and their structure-function relationships, *Front. Cell. Neurosci.*, **15**, 800313, https://doi.org/10.3389/fncel.2021.800313.
2. Sineshchekov, O. A., Govorunova, E. G., Der, A., Keszthelyi, L., and Nultsch, W. (1992) Photoelectric responses in phototactic flagellated algae measured in cell suspension, *J. Photochem. Photobiol. B Biol.*, **13**, 119-134, https://doi.org/10.1016/1011-1344(92)85051-u.
3. Sineshchekov, O. A., Jung, K.-H., and Spudich, J. L. (2002) Two rhodopsins mediate phototaxis to low- and high-intensity light in *Chlamydomonas reinhardtii*, *Proc. Natl. Acad. Sci. USA*, **99**, 8689-8694, https://doi.org/10.1073/pnas.122243399.
4. Govorunova, E. G., Jung, K.-W., Sineshchekov, O. A., and Spudich, J. L. (2004) *Chlamydomonas* sensory rhodopsins A and B: cellular content and role in photophobic responses, *Biophys. J.*, **86**, 2342-2349, https://doi.org/10.1016/s0006-3495(04)74291-5.
5. Deisseroth, K. (2015) Optogenetics: 10 years of microbial opsins in neuroscience, *Nat. Neurosci.*, **18**, 1213-1225, https://doi.org/10.1038/nn.4091.
6. Govorunova, E. G., Sineshchekov, O. A., Li, H., Wang, Y., Brown, L. S., Palmateer, A., Melkonian, M., Cheng, S., Carpenter, E., Patterson, J., Wong, G. K., and Spudich, J. L. (2021) Cation and anion channelrhodopsins: sequence motifs and taxonomic distribution, *mBio*, **12**, e0165621, https://doi.org/10.1128/mbio.01656-21.
7. Karpova, O. V., Vinogradova, E. N., and Lobakova, E. S. (2022) Identification of the channelrhodopsin genes in the green and cryptophytic algae from the White and Black seas, *Biochemistry (Moscow)*, **87**, 1187-1198, https://doi.org/10.1134/s0006297922100121.
8. Galietta, L. J., Haggie, P. M., and Verkman, A. S. (2001) Green fluorescent protein-based halide indicators with improved chloride and iodide affinities, *FEBS Lett.*, **499**, 220-224, https://doi.org/10.1016/s0014-5793(01)02561-3.
9. Hou, S. Y., Govorunova, E. G., Ntefidou, M., Lane, C. E., Spudich, E. N., Sineshchekov, O. A., and Spudich, J. L. (2012) Diversity of *Chlamydomonas* channelrhodopsins, *Photochem. Photobiol.*, **88**, 119-128, https://doi.org/10.1111/j.1751-1097.2011.01027.x.
10. Klapoetke, N. C., Murata, Y., Kim, S. S., Pulver, S. R., Birdsey-Benson, A., Cho, Y. K., Morimoto, T. K., Chuong, A. S., Carpenter, E. J., Tian, Z., Wang, J., Xie, Y., Yan, Z., Zhang, Y., Chow, B. Y., Surek, B., Melkonian, M., Jayaraman, V., Constantine-Paton, M., Wong, G. K., and Boyden, E. S. (2014) Independent optical excitation of distinct neural populations, *Nat. Methods*, **11**, 338-346, https://doi.org/10.1038/nmeth.2836.
11. Rozenberg, A., Oppermann, J., Wietek, J., Fernandez Lahore, R. G., Sandaa, R. A., Bratbak, G., Hegemann, P., and Béjà, O. (2020) Lateral gene transfer of anion-conducting channelrhodopsins between green algae and giant viruses, *Curr. Biol.*, **30**, 4910-4920, https://doi.org/10.1016/j.cub.2020.09.056.
12. Nagel, G., Ollig, D., Fuhrmann, M., Kateriya, S., Musti, A. M., Bamberg, E., and Hegemann, P. (2002) Channelrhodopsin-1: a light-gated proton channel in green algae, *Science*, **296**, 2395-2398, https://doi.org/10.1126/science.1072068.
13. Nagel, G., Szellas, T., Huhn, W., Kateriya, S., Adeishvili, N., Berthold, P., Ollig, D., Hegemann, P., and Bamberg, E. (2003) Channelrhodopsin-2, a directly light-gated cation-selective membrane channel, *Proc. Natl. Acad. Sci. USA*, **100**, 13940-13945, https://doi.org/10.1073/pnas.1936192100.
14. Govorunova, E. G., and Sineshchekov, O. A. (2023) Channelrhodopsins: from phototaxis to optogenetics, *Biochemistry (Moscow)*, **88**, 1555-1570, https://doi.org/10.1134/s000629792310015.
15. Hososhima, S., Ueno, S., Okado, S., Inoue, K., and Konno, M. (2023) A light-gated cation channel with high reactivity to weak light, *Sci. Rep.*, **13**, 7625, https://doi.org/10.1038/s41598-023-34687-7.

Publisher's Note. Pleiades Publishing remains neutral with regard to jurisdictional claims in published maps and institutional affiliations.